Space-Potential and Density Fluctuations in the ISX-B Tokamak

G. A. Hallock and A. J. Wootton
The University of Texas at Austin, Austin, Texas 78712

and

R. L. Hickok
Rensselaer Polytechnic Institute, Troy, New York 12181
(Received 22 December 1986)

The fluctuating plasma potential and electron density have been measured in Ohmic- and neutral-beam–heated tokamak discharges. Radial profiles are presented in the outer two-thirds of the plasma, and the $\mathbf{E}\times\mathbf{B}$ transport calculated. The transport is found to be an order of magnitude larger for beam-driven plasmas. Measurements indicate that the linearized Boltzmann equation is satisfied in the interior, but not at the plasma edge.

PACS numbers: 52.55.Fa, 52.35.Qz, 52.35.Ra, 52.70.Nc

It is widely believed that the broad-band fluctuations observed in tokamak discharges are the cause of anomalously large ($\gg$neoclassical) energy and particle transport near the plasma edge.[1] A detailed comparison with the predictions of various theories, such as those based on drift-wave instabilities, resistive ballooning modes, etc., has lacked a direct measurement of the interior plasma-potential fluctuations. This paper describes such measurements, which have been obtained with a heavy-ion beam probe on the ISX-B tokamak.

The impurity studies experiment-B (ISX-B) tokamak has major radius $R=93$ cm, average minor radius $\bar{a}=22$ cm, and is well documented.[2] The results presented here are for toroidal field $B_T=12$ kG, plasma current $I_p=130$ kA, and average plasma density $n_e\simeq 3\times 10^{13}$ cm^{-3}. Measurements are obtained for Ohmic heating only and for 800 kW of H^0 neutral beam injection (NBI) in the direction of the plasma current (coinjection). The working gas is deuterium, the plasma elongation is $\kappa\simeq 1.18$, and a beryllium rail limiter locates the top plasma edge at 24 cm.

We have recently described the ISX-B heavy-ion beam probe.[3] Here we inject $\simeq 25$ μA of Cs^{+1} at 125 keV, and detect Cs^{+2} secondaries in the analyzer. Measurements are highly localized in space, with a sample volume $\simeq 0.15$ cm^3. The analog measurement bandwidth is 500 kHz and the spatial uncertainty is ± 1 cm. Data are obtained for 1.5–2 ms at each measurement location in a single shot. The analyzer contains three entrance slits and associated detectors, allowing simultaneous measurements at three spatial points which are poloidally separated $\simeq 2$ cm in the plasma interior.

The energy of the Cs^{+2} secondary ions gives the sample-volume plasma potential, ϕ. The secondary ion current, $i_{\rm sum}$, gives the relative electron-density fluctuation

$$\frac{i_{\rm sum}-\langle i_{\rm sum}\rangle}{i_{\rm sum}}=\frac{\tilde{n}_e}{n_e}, \tag{1}$$

if the spatial correlation length of the turbulence is much less than the ion-beam path length to and from the sample volume, and if the Cs^{+1} ionization cross section is not temperature dependent. Correlation lengths are experimentally found to be a few centimeters, satisfying the first restriction. The second is satisfied for $T_e>50$ eV, corresponding to $\rho<0.95$, where ρ is the flux-surface radius normalized to the limiter.

Both potential and density measurements must be corrected for detector noise. The signal-to-noise ratio varies from 1 to 15, with smaller values for interior measurements because of attenuation of the Cs-ion beam. Extensive tests have shown the background noise to be uncorrelated with the localized measurement, and the noise is rms subtracted during data processing.[4] In addition, density fluctuations with wave number k comparable to the beam-probe sample length ($2\pi/k\lesssim l$) are measured as potential fluctuations. Modeling is difficult because of the complex geometry and dependency on the fluctuation spectra. Worst-case calculations indicate that the error in the measured $\tilde{\phi}$ is less than 50%.

Data from each radial measurement location are divided into five or more nonoverlapping 0.256-ms (256 data-point) intervals. Each interval is Fourier analyzed, and the results ensemble averaged.[5] Typical spectra, shown in Fig. 1, are similar for all radial positions for both Ohmic heating and NBI. The rms fluctuation levels presented here are integrated from 50 to 500 kHz, which avoids MHD oscillations ($f<50$ kHz) and contains most of the power from the microscopic plasma turbulence.

For both NBI and Ohmic heating only, $\tilde{n}/n$ is $\simeq 1\%$ in the plasma interior, as shown in Fig. 2. Near the plasma edge, fluctuation levels are much larger, and also beam heating increases the fluctuation level about a factor of 2 above that for Ohmic heating only. For Ohmic discharges, $\tilde{n}/n$ reaches a peak level of $\simeq 7\%$ at $\rho=1$. For neutral-beam injection $\tilde{n}/n\simeq 14\%$ at the limiter. These data are consistent with scattering measurements on oth-

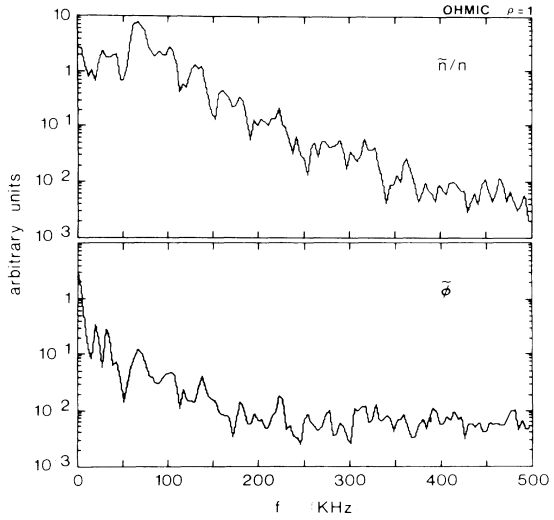

FIG. 1. Typical autopower spectra of $\tilde{n}/n$ and $\tilde{\phi}$.

er tokamaks[6] and probe measurements in ISX-B.[7]

Drift-wave, or density-gradient-driven, turbulence is expected to saturate at the "mixing-length level" $\tilde{n}/n \sim 1/\langle k_\perp \rangle L_n \sim (3\text{-}10)\rho_s/L_n$, where $k_\perp$ is the mean wave number, $L_n = -[d(\ln n)/dr]^{-1}$ is the density-gradient scale length, and $\rho_s = \rho_i (T_e/T_i)^{1/2}$ is the ion gyroradius ρ_i evaluated at the electron temperature.[1] The n and T_e profiles are measured by Thomson scattering and edge Langmuir probes,[2,7] with central and edge values given in Table I. Results indicate $\tilde{n}/n \sim \rho_s/L_n$ for $\rho < 0.8$, as shown in Fig. 2(c). At the plasma edge the increase in $\tilde{n}/n$ is not followed by ρ_s/L_n.

TABLE I. Central ($\rho=0$) and edge ($\rho=1$) values of the electron temperature and density.

Heating	T_{e0} (eV)	T_{ea} (eV)	n_{e0} (cm^{-3})	n_{ea} (cm^{-3})
Ohmic	600	20	4×10^{13}	2×10^{12}
Coinjection	800	40	4×10^{13}	1×10^{13}

At all radial positions $\tilde{\phi}$ is larger for beam-injected plasmas, as shown in Fig. 3. For $\rho < 0.8$, rms levels are $\tilde{\phi} \simeq 2\text{-}4$ V for Ohmic heating and 5–10 V for beam injection. Edge amplitudes are $\tilde{\phi} \simeq 12$ V rms for Ohmic

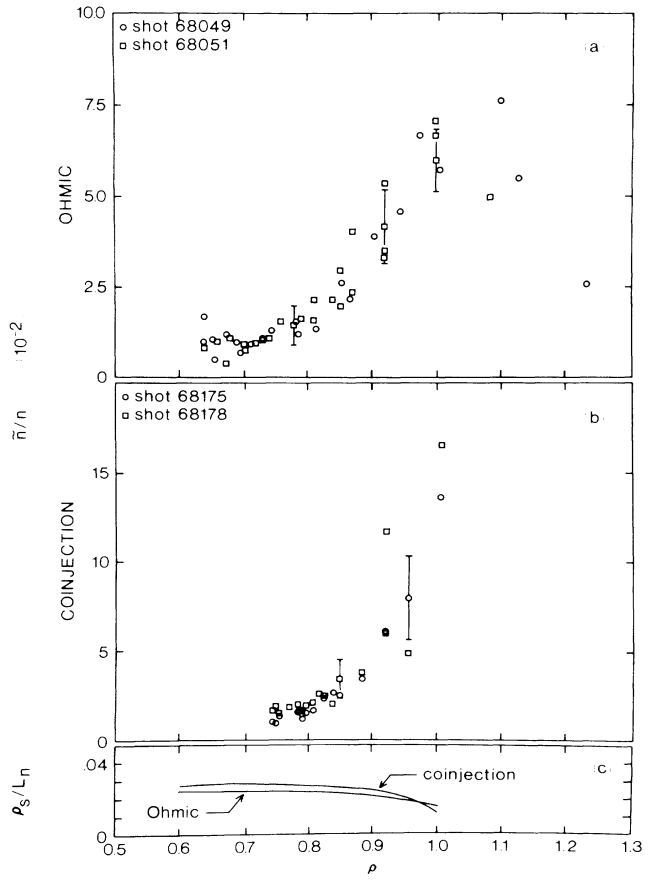

FIG. 2. Radial distribution of the relative density fluctuation level $\tilde{n}/n$, with (a) Ohmic heating only and (b) 800-kW neutral-beam coinjection; (c) the mixing-length limit ρ_s/L_n.

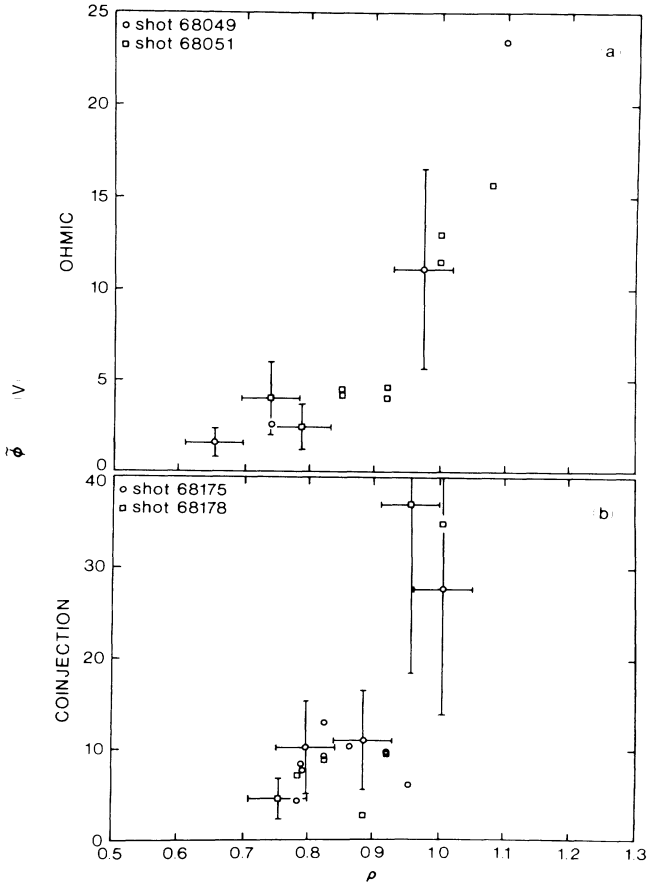

FIG. 3. Radial distribution of the space-potential fluctuation level for (a) Ohmic heating and (b) neutral-beam injection.

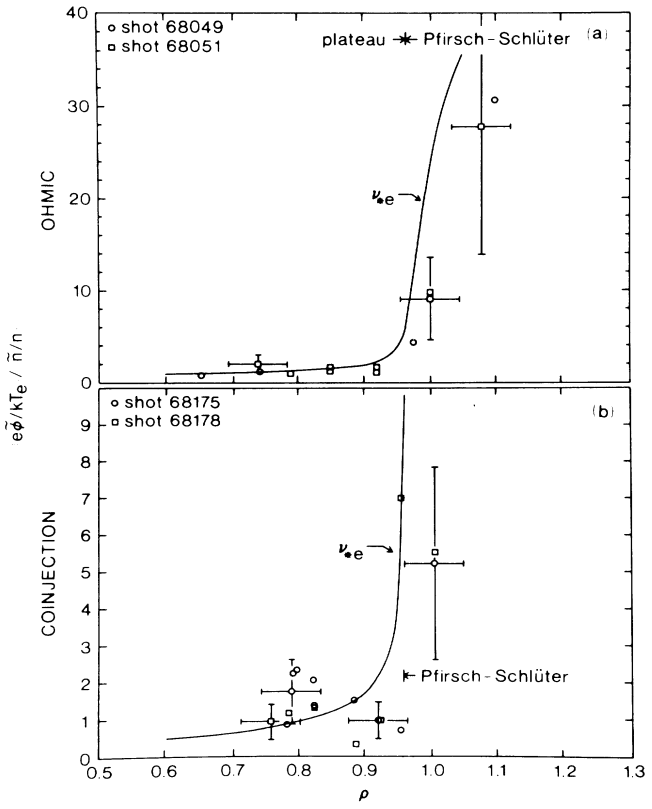

FIG. 4. The normalized potential/density fluctuation levels and the electron collisionality ν_{*e}.

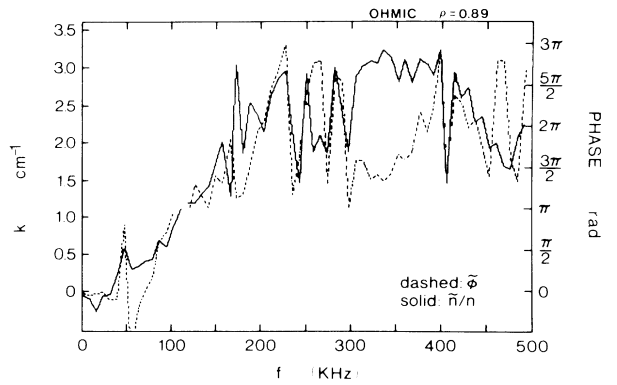

FIG. 5. Wave-number spectra of $\tilde{\phi}$ and $\tilde{n}/n$. For $f \lesssim 250$ kHz high coherency (>0.5) is obtained between measurement locations.

heating and $\simeq 30$ V rms with neutral-beam heating. These data are in good agreement with edge ($\rho > 0.95$) potential measurements obtained with Langmuir probes on ISX-B and similar tokamaks.[7]

The ratio $(e\tilde{\phi}/kT_e)/(\tilde{n}/n)$ is shown in Fig. 4, where k is the Boltzmann constant. Also shown is the electron collisionality, $\nu_{*e} = \nu_{\text{eff}}/\nu_b$, where ν_{eff} is the collision frequency for the scattering of electrons out of trapped phase space, and ν_b is the bounce frequency of trapped electrons. For $\rho < 0.95$, the linearized Boltzmann relation $(e\tilde{\phi}/kT_e)/(\tilde{n}/n) \sim 1$ is satisfied within the measurement uncertainty. Near the plasma edge $e\tilde{\phi}/kT_e \gg \tilde{n}/n$. The data support drift-wave turbulence, or another instability requiring an adiabatic response, in the interior, and a larger-amplitude edge instability with $e\tilde{\phi}/kT_e \gg \tilde{n}/n$.

The radial $(\mathbf{E}\times\mathbf{B})$-driven particle flux, $\Gamma_{\mathbf{E}\times\mathbf{B}}(\omega)$, resulting from the density and potential fluctuations is given by

$$\Gamma_{\mathbf{E}\times\mathbf{B}}(\omega) = \frac{k_\theta(\omega)\,|P_{\tilde{n}/n,\tilde{\phi}}(\omega)|\,n\sin[\alpha_{\tilde{n}/n,\tilde{\phi}}(\omega)]}{B_T}, \quad (2)$$

where $P_{\tilde{n}/n,\tilde{\phi}}$ is the cross-amplitude between $\tilde{n}/n$ and $\tilde{\phi}$, k_θ is the poloidal wave-number spectrum of the potential fluctuations, α is the phase between $\tilde{n}/n$ and $\tilde{\phi}$, and the electrostatic approximation $\mathbf{E} = -\nabla\phi$ is used.[5] The wave number is obtained from the cross-phase between the simultaneous spatial measurements, as shown in Fig. 5 for $\rho = 0.89$. At the plasma edge the sample volumes become radially separated, in addition to their poloidal separation. To account for this, we assume $k_r \sim k_\theta$, as determined by probe measurements.[1] Within measurement uncertainty, k is unchanged with spatial location and neutral-beam heating, and the phase difference between $\tilde{\phi}$ and $\tilde{n}/n$ is $\simeq 20°$. Equation (2) is integrated from 45 to 250 kHz, which accounts for essentially all of the particle flux. Doppler shifts in the spectra from NBI-induced toroidal rotation are negligible for $\rho > 0.75$.

The total particle flux, shown in Fig. 6, is an order of magnitude larger for beam-heated discharges, $\simeq 5\times10^{16}$ cm^{-2} s^{-1} compared to $\simeq 5\times10^{15}$ cm^{-2} s^{-1} for Ohmic heating at $\rho = 1$. In both cases, the flux increases about a factor of 5 from the most interior measurement points to the limiter radius, and is measured to be outward in the laboratory frame. The particle-confinement times ($\sim \bar{n}\bar{a}/2\Gamma$) inferred are 60 ± 30 ms (Ohmic) and 7 ± 3 ms (NBI). The latter is in reasonable agreement with global estimates of $\simeq 3$ ms.[7] The Ohmic value is larger than expected, although no data are available for the exact conditions.

Gentle has shown that it is necessary to invoke inward convection, as well as diffusion, to model equilibrium and time-dependent density profiles in Ohmic discharges, $\bar{\Gamma} = -D\nabla n + n\mathbf{v}$, with D the diffusion coefficient and $\mathbf{v}$ a convection velocity.[8] For discharges similar to those discussed here, and $\rho < 0.8$ (no ionization source of particles, $\Gamma \simeq 0$), $|D\nabla n| \simeq |n\mathbf{v}| \simeq 2\times10^{16}$ cm^{-2} s^{-1}. We measure $\Gamma_{\mathbf{E}\times\mathbf{B}} \ll 2\times10^{16}$ for $\rho \simeq 0.75$. This implies that the electrostatic turbulence may be responsible for both the diffusion and the convection in the interior, or neither.

Power-balance studies for these discharges show net unaccounted for power (from conduction and convection) of $\simeq 70$ kW for Ohmic heating and $\simeq 400$ kW with

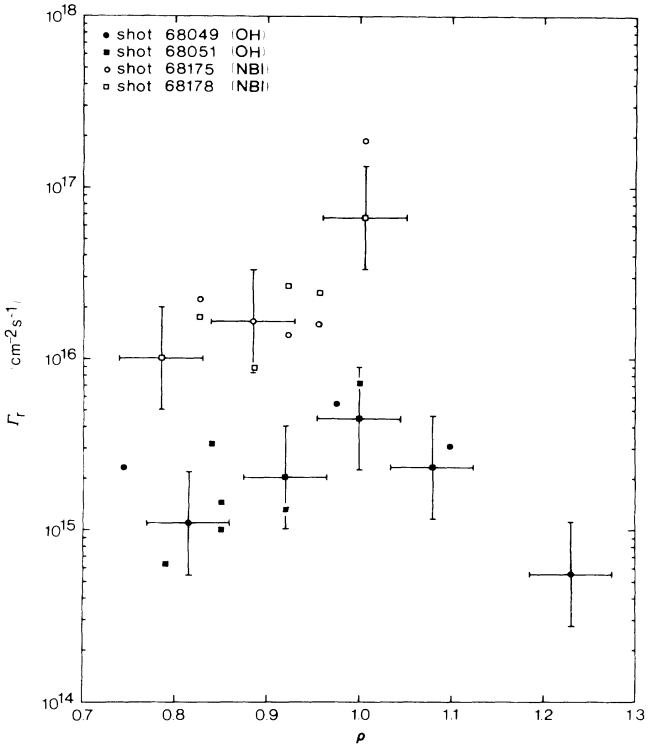

FIG. 6. Radial ($\mathbf{E}\times\mathbf{B}$)-driven particle flux (OH=Ohmic heating).

NBI.[2] With the assumption that $\Gamma_{\mathbf{E}\times\mathbf{B}}(\rho=1)$ is uniform over the entire plasma surface S, the convected $\mathbf{E}\times\mathbf{B}$ power loss ($5kT_e\Gamma S/2$) is $\simeq$3.5 kW for Ohmic heating and $\simeq$65 kW for beam injection.

In summary, we have directly measured the fluctuating plasma density and potential in the outer two-thirds of the ISX-B plasma. The $\mathbf{E}\times\mathbf{B}$ transport is an order of magnitude larger for neutral-beam–driven plasmas than for Ohmic heating only. Our data indicate low-amplitude turbulence in the plasma interior, with the linearized Boltzmann equation satisfied, and a much higher turbulence level, which is not likely drift-wave turbulence, at the plasma edge. That the shape of $k(\omega)$, $\tilde{\phi}(\omega)$, and $\tilde{n}/n(\omega)$ does not change with NBI suggests that the basic nature of the turbulence does not change, merely the amplitude. Simple calculations indicate that the fluctuation-induced power loss is significant.

The authors would like to acknowledge the Fusion Energy Division of the Oak Ridge National Laboratory for their strong support of this project. We would like to particularly thank J. Mathew and P. H. Edmonds for their assistance during the experiments, S. G. Duran who developed much of the software used in the data processing, and Ch. P. Ritz, P. M. Schoch, J. C. Forster, and T. Crowley for valuable discussions. This work was sponsored by the U.S. Department of Energy.

[1]P. C. Liewer, Nucl. Fusion **25**, 543 (1985).

[2]P. K. Mioduszewski *et al.*, Nucl. Fusion **26**, 1171 (1986).

[3]G. A. Hallock *et al.*, Phys. Rev. Lett. **56**, 1248 (1986).

[4]G. A. Hallock, University of Texas at Austin Report No. UT/CFE-PR-3, 1986 (unpublished).

[5]E. J. Powers, Nucl. Fusion **14**, 749 (1974).

[6]T. Crowley and E. Mazzucato, Nucl. Fusion **25**, 507 (1985).

[7]A. J. Wootton *et al.*, Oak Ridge National Laboratory Report No. ORNL/TM-9305, 1986 (unpublished).

[8]K. W. Gentle, in *Proceedings of the Thirteenth European Conference on Controlled Fusion and Plasma Physics, Schliersee, West Germany, 1986*, edited by G. Brifford and M. Kaufmann (European Physical Society, Petit-Lancy, Switzerland, 1986), p. 244.